Philosophical Magazine A
Publication details, including instructions for authors and subscription information:
http://www.tandfonline.com/loi/tpha20

Collective evolution characteristics and computer simulation of short fatigue cracks

Youshi Hong [a] , Ziyan Gu [a] , Biao Fang [a] & Yilong Bai [a]
[a] Laboratory for Nonlinear Mechanics of Continuous Media, Institute of Mechanics, Chinese Academy of Sciences , Beijing, 100080, PR China
Published online: 20 Aug 2006.

To cite this article: Youshi Hong , Ziyan Gu , Biao Fang & Yilong Bai (1997) Collective evolution characteristics and computer simulation of short fatigue cracks, Philosophical Magazine A, 75:6, 1517-1531, DOI: 10.1080/01418619708223741

To link to this article: http://dx.doi.org/10.1080/01418619708223741

PHILOSOPHICAL MAGAZINE A, 1997, VOL. 75, NO. 6, 1517–1531

Collective evolution characteristics and computer simulation of short fatigue cracks

By YOUSHI HONG†, ZIYAN GU, BIAO FANG and YILONG BAI

Laboratory for Nonlinear Mechanics of Continuous Media, Institute of Mechanics, Chinese Academy of Sciences, Beijing 100080, PR China

[*Received 15 November 1995 and accepted in revised form 12 October 1996*]

ABSTRACT

Fatigue testing was conducted using a kind of triangular isostress specimen to obtain the short-fatigue-crack behaviour of a weld low-carbon steel. The experimental results show that short cracks continuously initiate at slip bands within ferrite grain domains and the crack number per unit area gradually increases with increasing number of fatigue cycles. The dispersed short cracks possess an orientation preference, which is associated with the crystalline orientation of the relevant slip system. Based on the observed collective characteristics, computer modelling was carried out to simulate the evolution process of initiation, propagation and coalescence of short cracks. The simulation provides progressive displays which imitate the appearance of experimental observations. The results of simulation indicate that the crack path possesses a stable value of fractal dimension whereas the critical value of percolation covers a wide datum band, suggesting that the collective evolution process of short cracks is sensitive to the pattern of crack site distribution.

§ 1. INTRODUCTION

The research on the initiation and propagation of short fatigue cracks in metals and alloys has received increasing attention because the subject has great importance both for the distinct behaviour of short cracks, which cannot be interpreted by conventional theories, and for engineering interests since the stage of short-crack damage may occupy a large portion of total fatigue life.

The anomalous growth phenomenon is one of the distinct features for short cracks and the study of this has attracted many investigations in the interdisciplinary field between materials physics and mechanics. For instance, short cracks in aluminium alloys and structural steels were observed to grow at rates faster than those predicted by linear elastic fracture mechanics (Lankford 1982, Romaniv, Siminkovich and Tkach 1982, Tanaka, Hojo and Nakai 1983). One explanation for this is that the size of the plastic zone associated with short cracks is several times greater than that of a large crack with a similar driving force (Lankford, Davidson and Chan 1984). In such observations, a resulting curve was readily plotted through the monitoring of a single short crack and the replica technique was commonly used in the crack trace observation.

A number of investigations have focused on the microstructurally short cracks, namely where the crack length is comparable with the size of microstructural unit of the material concerned (e.g. the grain size in steel), for which the effect of micro-

†Author for correspondence.

structure on short-crack behaviour plays a dominant role in fatigue damage. Accelerations and decelerations of crack growth rate in this regime are attributed to the interaction of the crack tip plastic zone with microstructural barriers to plastic flow, which produces the oscillating pattern of crack velocity (Lankford 1982, Zurek, James and Morris 1983, Fathulla, Weiss and Stickler 1986). To describe the microstructural effect on the growth pattern of short cracks, Navarro and Rios (1988a, b, c) developed a model, which predicted the trend that fatigue threshold stress decreased with the increase in crack length and, more significantly, described the intermittent pattern of short-crack growth. Again, the analysis and the derivation of the model were based on the behaviour of a single crack.

On the other hand, several investigations have noticed that the initiation and the propagation of short fatigue cracks in some metallic materials present collective evolution characteristics (Price 1988, Price and Henderson 1988, Price and Houghton 1988, Hong, Lu and Zheng 1989, 1991). The number of short fatigue cracks gradually increases with increasing number of fatigue cycles (Price 1988, Hong *et al.* 1989). The orientation of short cracks that initiate at matrix grains possesses a preference related to the orientation of corresponding slip system (Hong *et al.* 1991). However, only a few published articles with quantitative measurements and analysis for dispersive short cracks are available because of the difficulties in both experimental observations and statistical evaluation.

To tackle this problem, Suh *et al.* (1992) performed a statistical simulation on the evolution of dispersive short cracks in AISI 316 stainless steel, showing two-dimensional graphical displays of short-crack development and being applied to fatigue life prediction. In their simulation, Suh *et al.* took into account several factors that affected short-crack development, such as location and distribution patterns, initiation and growth feature, crack density, distribution of crack length, and the incremental of average crack length, etc. However, two factors with considerable importance, namely the presence of microstructural barriers and short crack orientation, were not considered in that simulation. These two factors have been identified as essential effects on the conditions for connection and interaction between short cracks.

In this paper, quantitative measurements of crack density per unit area and crack orientation distribution of a weld low-carbon steel are illustrated. The preference of crack orientation is further discussed from the viewpoint of slip system activation. An attempt at computer simulation is made to model the collective evolution process of short cracks, in which both the effects of grain boundaries and the distribution of crack orientation are taken into account.

§ 2. Experimental procedure and results

The material used in this investigation is a weld low-carbon steel with the following chemical composition: C, 0·12 wt%; Si, 0·55 wt%; Mn, 0·97 wt%; P, 0·025 wt%; S, 0·012 wt%; Fe, balance. The material was normalized so that the microstructure consisted of ferrite and pearlite. The average ferrite grain size is 22 μm and the pearlite percentage is 16%. The yield stress of the material σ_y is 310 MPa and the ultimate strength is 550 MPa. A kind of triangular specimen (fig. 1) was used in fatigue testing, for which the surface tensile stress σ_{max} was maintained constant over the gauge length when the specimen is subjected to a given loading (Hong, Lu and Zheng 1990). Fatigue testing was performed at a frequency between 10 and 12 Hz with stress ration $R = -1$ and $\sigma_{max} = (0{\cdot}8\text{–}1{\cdot}7)\sigma_y$. The cycling was per-

Fig. 1

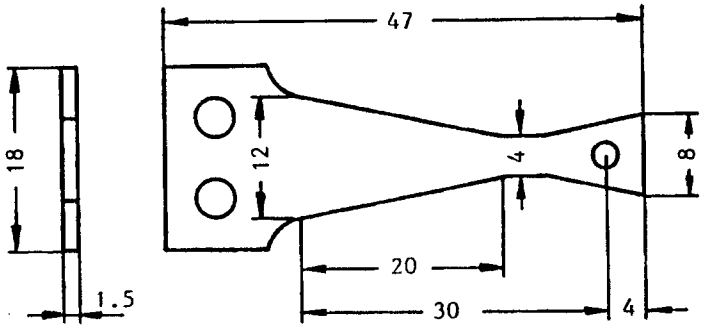

Schematic of triangular specimen (dimensions in millimetres).

iodically interrupted and the specimen was observed with an optical microscope with polarized illumination. The photographs taken of the same field traced the initiation and development process of short cracks. The data on short-crack evolution were measured with an image analyser equipped with an optical microscope. Figure 2 shows the photographs of the same field on the surface of a pre-polished but unetched specimen at the stress level $\sigma_{max} = 1{\cdot}1\sigma_y$. The formation of short cracks was first observed after several thousand cycles of fatigue testing (fig. 2(*a*)). The observations from the surface of etched specimen revealed that short cracks originated from slip bands of ferrite grains (fig. 3). A short crack could grow within a ferrite grain until it reached a grain boundary. Simultaneously, the number of short cracks gradually increased with increasing number of fatigue cycles (figs. 2 and 3). At some locations, the propagation of an isolated crack terminated at grain boundary could either proceed through coalescence with a nearby short crack or grow into the adjacent grain itself when the stress level was large enough to overcome the barrier.

Fig. 2

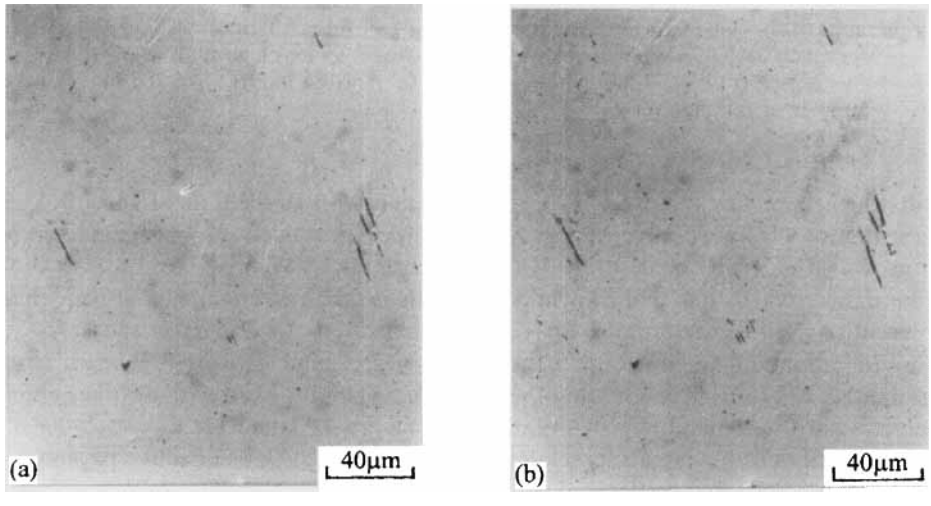

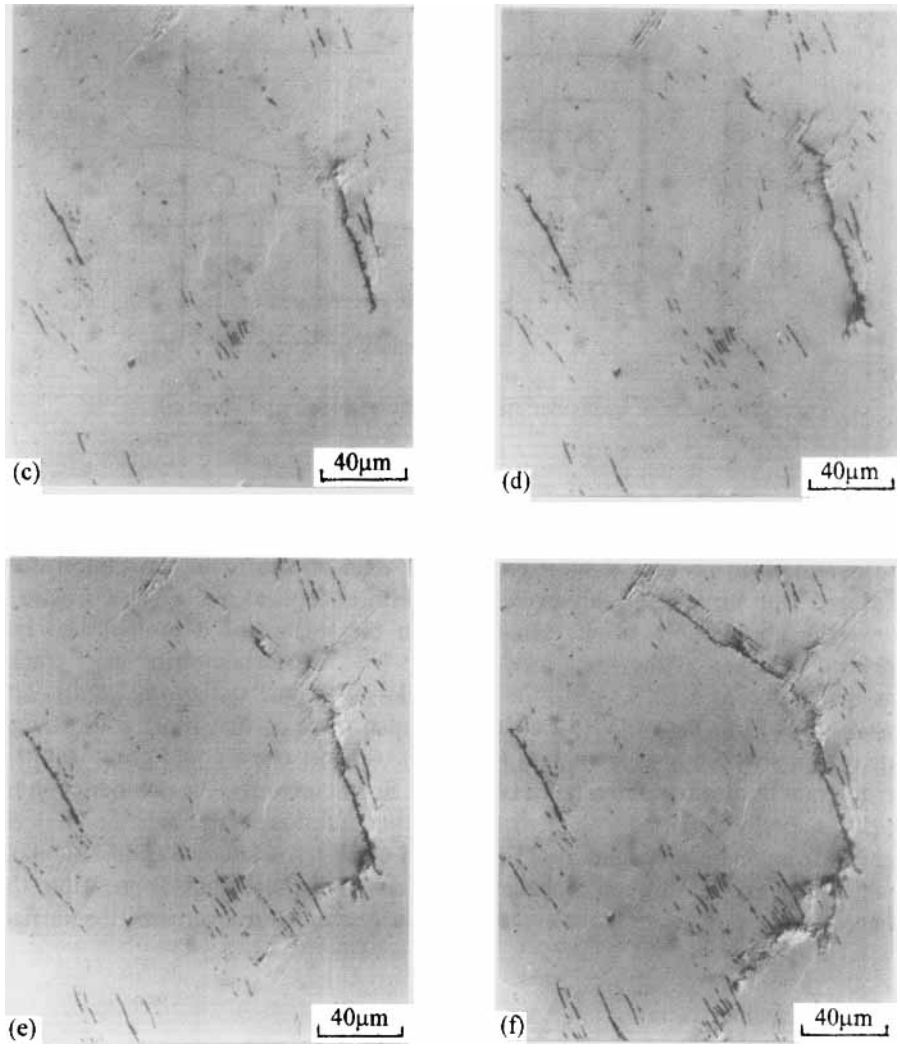

Photographs of the same field showing the progression of short fatigue cracks on an unetched specimen at $\sigma_{max} = 1{\cdot}1\sigma_y$ (transverse axis parallel to tensile stress): (*a*) $n = 9900$; (*b*) $n = 29\,700$; (*c*) $n = 69\,300$; (*d*) $n = 148\,500$; (*e*) $n = 168\,300$; (*f*) $n = 207\,900$. (n is the number of fatigue cycles.)

Consequently, a few main cracks appeared, each with the length of several grain sizes. Figure 4 is an example of a growing main crack, which may propagate either by growth itself or by coalescence with adjacent cracks. Figures 2 and 4 also show some cracks which had halted while the main crack was advancing. From these observations, the growth rate for some specified cracks could be measured to show the anomalous behaviour in the short-crack regime. However, when a crack terminated at a barrier or, on the other extreme, when it linked with another crack, then it is hard to define the growth rate of such a crack. Therefore the crack density per unit area and the average crack length are considered to be effective parameters in the description of short fatigue cracks. With regard to this, the result in fig. 5 is

Fig. 3

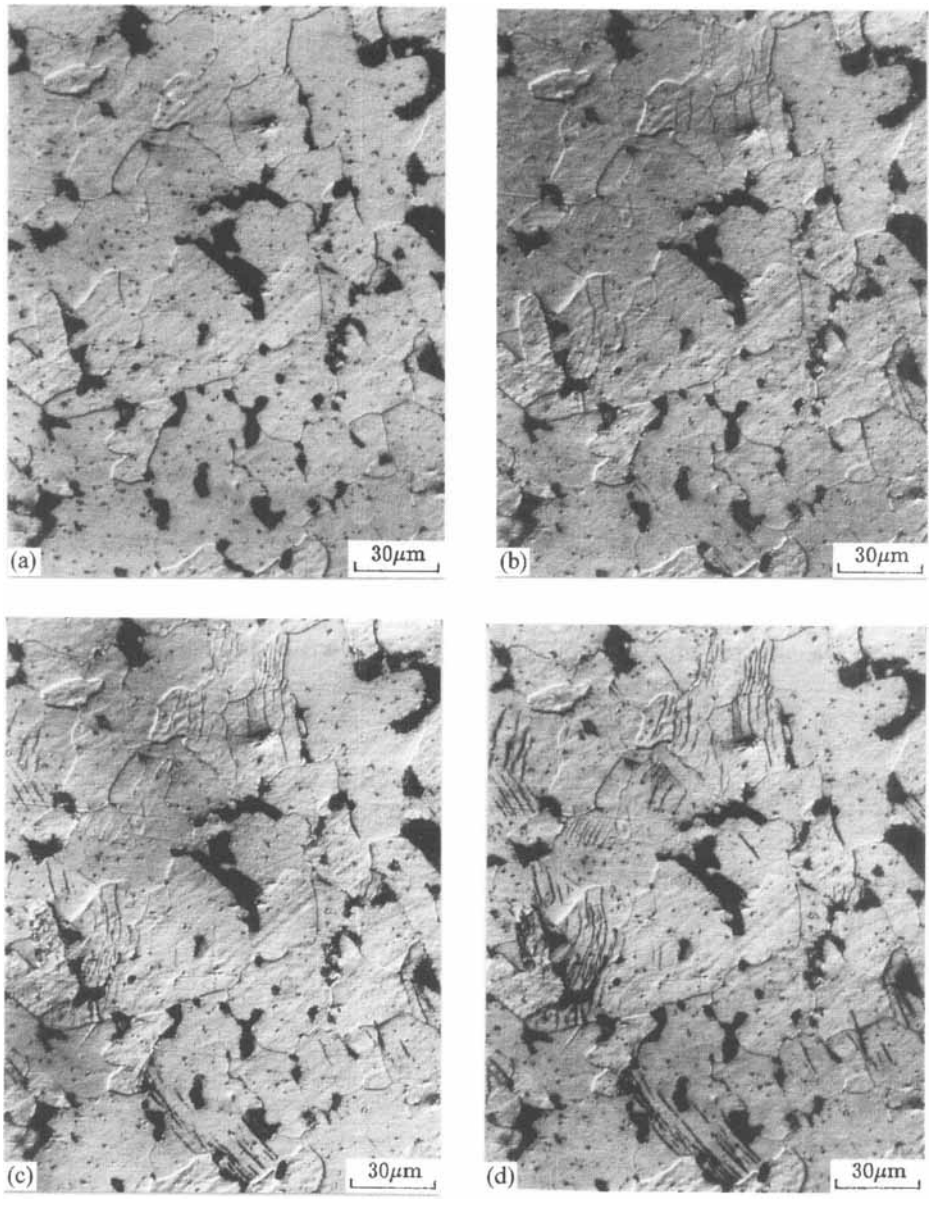

Photographs of the same field showing the progression of short fatigue cracks on an etched specimen at $\sigma_{max} = 1{\cdot}2\sigma_y$ (transverse axis parallel to tensile stress): (*a*) $n = 0$; (*b*) $n = 6000$; (*c*) $n = 30\,000$; (*d*) $n = 61\,000$.

obtained to show the increase in cumulative crack density per unit area as a function of crack length and fatigue cycles. This figure is a typical example of a specimen subjected to cycling at $\sigma_{max} = 1{\cdot}7\sigma_y$, where each curve was obtained from the measurements, using an image analyser, on 31 identified fields with each field size of 150 μm × 150 μm.

Fig. 4

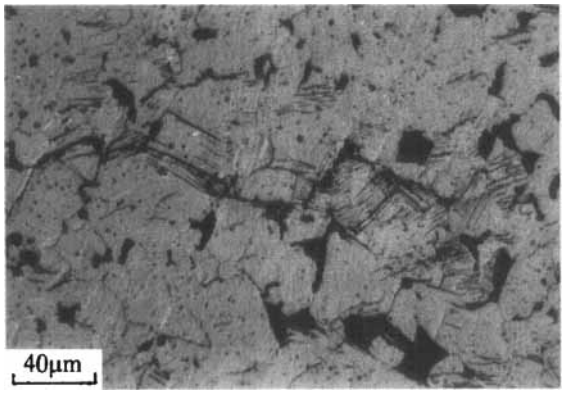

A main crack running through several ferrite grains after $n = 230\,000$ at $\sigma_{max} = 1{\cdot}2\sigma_y$ (vertical axis parallel to tensile stress).

Figure 5 quantitatively demonstrates that the number of short cracks per unit area progressively increases with increasing number of fatigue cycles, and the average crack length presents little change. (Note that, when the value of cumulative crack number is half its total, the corresponding crack size is the mean length). From the result in fig. 5 together with figs. 2 and 3, one may obtain the impression that the progression of short-crack damage is in a collective way which is marked by the gradual increase in crack number on specimen surface.

After the completion of fatigue testing, some specimens were longitudinally sectioned and were then mounted, ground and polished. The prepared profile samples were examined by optical and scanning electron microscopy.

Fig. 5

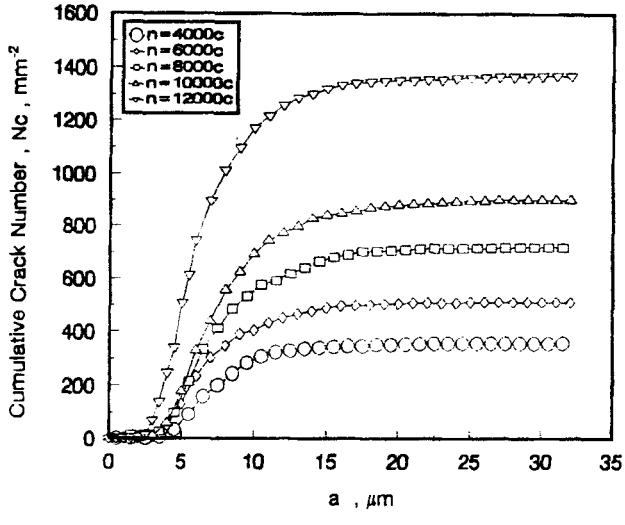

Cumulative crack number against crack length at different numbers of fatigue cycles.

§ 3. Orientation characteristics of short cracks

As mentioned above, short cracks initiate from slip bands of ferrite grains. Thus the orientation of a short crack is dependent on the relevant slip system. For convenience in the discussion, we define, as shown in fig. 6, (*a*) the angle between a short crack trace on specimen surface and tensile stress direction as α, and (*b*) the angle between a short-crack trace at profile plane and tensile stress direction as β. A developed short crack can be seen on both the surface and the profile of specimen, and a pair of α and β values can be measured, which described the orientation of the crack.

Macroscopically, the distribution of short cracks at initiation within the specimen gauge length where a constant surface tensile stress prevailed was nearly uniform. Microscopically, however, short cracks did not initiate evenly among the ferrite grains. At the early stage, short cracks appeared in only a few ferrite grains, and the orientation of these cracks tended to be perpendicular to the surface tensile stress or α tended to $\pi/2$ (fig. 3(*b*)). Subsequently, new cracks initiated both in the grains with prior cracks and in some others without previous cracking. The short cracks formed later lay in directions gradually deviating from the axis perpendicular to the tensile stress. Eventually, the distribution of angles α covered the range from 90° to 45° (figs. 2 and 3). Figure 7(*a*) is a result of measurements shown in the variation in specific crack number with angle α.

On the other hand, the examinations from profile samples indicated that the main cracks, each with a length of several grain sizes, were observed with their depth varying from 10 to 100 μm. The value of angle β was measured from scanning electron micrographs taken of profile samples. It is noted that angle β is also preferentially $45 \pm 15°$ or $135 \pm 15°$ and fig. 7(*b*) shows the result of the measurements.

On the basis of the above observations, the following two cases are discussed. For *case I* it is assumed firstly that the short crack propagates along slip plane, and secondly the crack trace observed on the profile of specimen is slip direction. Thus, one may use the following equation to calculate the orientation factor S of the crack plane determined by a pair of α and β values:

Fig. 6

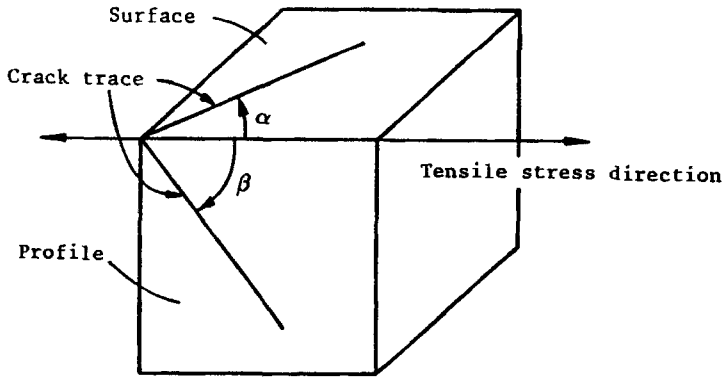

Schematic diagram of crack traces on specimen surface and profile.

Fig. 7

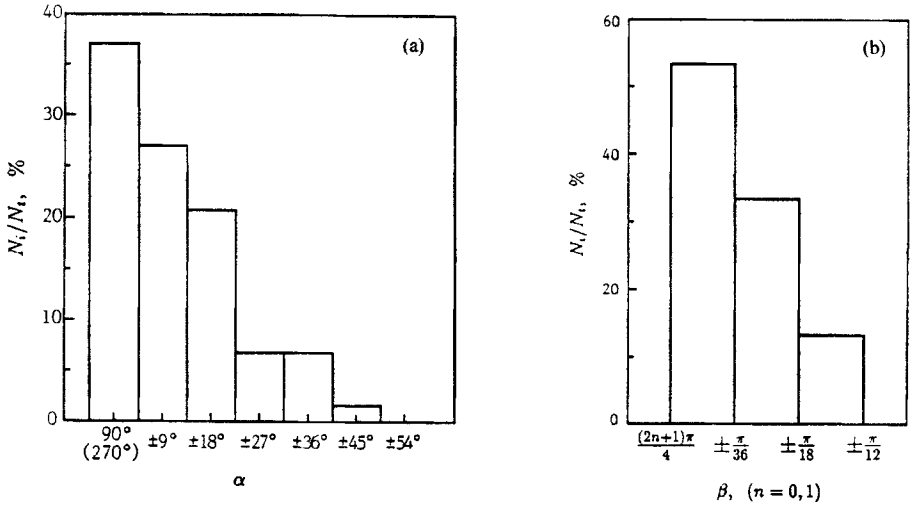

Measurements of crack orientation: (*a*) distribution of angle α; (*b*) distribution of angle β, with N_i being the number of cracks at grade i and N_t being the total number of cracks.

$$S = \cos\phi\cos\lambda = \frac{\mathbf{r}\cdot\mathbf{T}}{|\mathbf{r}||\mathbf{T}|}\cos\beta, \tag{1}$$

where ϕ is the angle between the normal to the slip plane and the tensile stress direction, λ is the angle between the slip direction and the tensile axis, $\mathbf{r}$ is the unit vector along the normal of slip plane and $\mathbf{T}$ is the unit vector of tensile stress direction. Referring to fig. 6, we have $\mathbf{r} = (1, -\cot\alpha, \cot\beta)$ and $\mathbf{T} = (1, 0, 0)$, such that

$$S = \frac{\cos\beta}{(\cot^2\alpha + \cot^2\beta + 1)^{1/2}}. \tag{2}$$

For *case II* it is assumed firstly that the short crack propagates along the slip plane, and secondly that the slip direction lies in the plane determined by a set of α and β and is parallel to the normal of surface crack trace defined by α. For this situation, one may write a unit vector along the slip direction to be $\mathbf{v} = (\sin^2\alpha, -\sin\alpha\cos\alpha, -\tan\beta)$. Then

$$\cos\lambda = \frac{\sin^2\alpha}{(\sin^2\alpha + \tan^2\beta)^{1/2}}. \tag{3}$$

Hence,

$$S = \frac{1}{(\cot^2\alpha + \cot^2\beta + 1)^{1/2}} \frac{\sin^2\alpha}{(\sin^2\alpha + \tan^2\beta)^{1/2}}. \tag{4}$$

Now, we can discuss the orientation preference of short cracks in terms of S for concerned slip systems. From symmetry consideration, we took $\pi/6 \leqslant \alpha \leqslant \pi/2$ and $\pi/8 \leqslant \beta \leqslant 3\pi/8$ in the estimation. Figures 8 (*a*) and (*b*) are the results of three-dimen-

Fig. 8

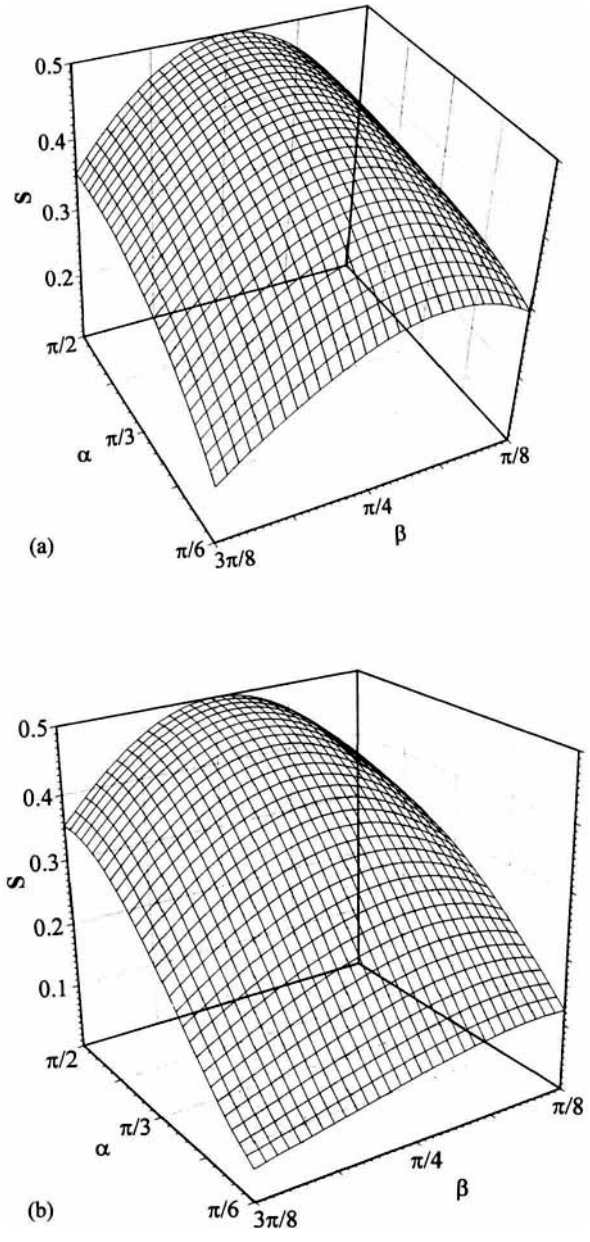

Three-dimensional construction of orientation factor distribution: (*a*) case I; (*b*) case II.

sional construction showing the value of S as a function of α and β for the two cases respectively. It is seen that the variations in S with α and β are similar in both cases. When $\alpha = \pi/2$, the value of S is symmetrical with β and reaches its maximum, that is $S = 0{\cdot}5$, when $\beta = \pi/4$. The value of S declines asymmetrically along the directions of $\pi/4 < \beta < \pi/4$ and $\alpha < \pi/2$, with a faster decreasing rate towards $\beta > \pi/4$. The

attenuation trend of S is more obvious in case II. The larger the value of the orientation factor, the more prone is the relevant system to slip; therefore the system is more active in the initiation of short cracks. The calculation results of orientation factor provide an explanation for the fact that the preference of short-crack orientation is $\alpha \to \pi/2$ with $\beta \to \pi/4$.

As short cracks originate from slip bands of ferrite grains whose crystalline orientation is randomly distributed, and the activation of a slip system is directly associated with the resolved shear stress on the slip plane, therefore the orientation of dispersive short cracks is governed by both the randomness of grain orientation and the tensile stress direction. As a result, the orientation of randomly distributed short cracks possesses a definite preference, which is regarded as another distinct feature of collective evolution characteristics for short cracks.

§ 4. Computer simulation of the progression of short cracks

The above experimental results have revealed that, for low-carbon steel, the development of short fatigue cracks is an evolution process with a collective response of dispersed cracks. Computer programs were therefore developed to simulate the evolution process of short cracks, in which the effect of grain boundaries on short-crack growth and the preference of short-crack orientation were taken into account. The hexagonal shape of grain arrangement was constructed as the initial background. Two types of crack orientation distribution were considered. For type I, all cracks on initiation are perpendicular to the tensile stress. Such a crack may deflect only when it links with an adjacent crack. For this type, the width δ of crack, is introduced into the simulation. In practice, $\delta = 0{\cdot}02a$, with a being the crack length, which is an approximation from the strip yield model of crack tip opening. In type II, the surface angle α of each crack is distributed in a stochastic way according to the experimental measurements and the probability of angle α is assigned by the estimation of case II. Note that the change in angle β does not affect the variation in S with angle α much and, when $\beta = \pi/4$, the shape of the curve for S against α is more reflected in the measurements of α against N_i/N_t (fig. 7 (*a*)). When $\beta = \pi/4$, eqn. (4) reduces to

$$S(\alpha) = \frac{1}{(\cot^2 \alpha + 2)^{1/2}} \frac{\sin^2 \alpha}{(\sin^2 \alpha + 1)^{1/2}}. \tag{5}$$

Thus the probability $Q(\Delta\alpha)$, that the orientation angle α occurs for a crack, is

$$Q(\Delta\alpha) = \int_{\alpha_1}^{\alpha_2} S(\alpha)\, d\alpha, \tag{6}$$

where $\Delta\alpha$ is given as $2{\cdot}5^\circ$ and the range of α is $90 \pm 45^\circ$. In addition to the above consideration for crack orientation, the following stipulations were also made in the simulation.

(*a*) The location for crack initiation was randomly distributed.
(*b*) The length of each crack on initiation was randomly assigned, with the upper bound being the grain size.
(*c*) 20 individual cracks were produced at each time step and each crack formed extended at a speed proportional to its length.

(*d*) Each crack could grow until it touched a grain boundary and, when the crack length was greater than three times the grain size, then the crack could grow across grain boundary itself.

(*e*) When the distance x between two crack tips satisfied the following criterion, coalescence between two cracks would occur:

$$x < a_1 + a_2 - (a_1^2 + a_2^2)^{1/2}, \tag{7}$$

with a_1 and a_2 being the lengths of cracks respectively.

Equation (7) is a quantitative expression obtained by estimation based on the view that the critical condition for two-crack coalescence is when the potential energy increment due to the total crack $(a_1 + a_2 + x)$ is less than the sum of the energy created by the two separate cracks (a_1 and a_2).

Figure 9 shows the different stages of a simulation with vertical crack orientation. The segments of crack path with an oblique angle are produced by crack linkage, to which the criterion of eqn. (7) is applied. Figure 10 shows the results of another simulation, in which the crack orientation is dispersed within an angle range of $90 \pm 45°$ with the probability controlled by eqn. (6). The displays of the two examples imitate the observed collective evolution process of crack initiation, growth and coalescence.

Two parameters are evaluated for the simulation results. The first is fractal dimension D_F of crack path that causes final fracture (cross-section crack). The following definition for D_F (Pande *et al.* 1987) is used:

$$L = L_0 \eta^{-(D_F - 1)} \tag{8}$$

or

Fig. 9

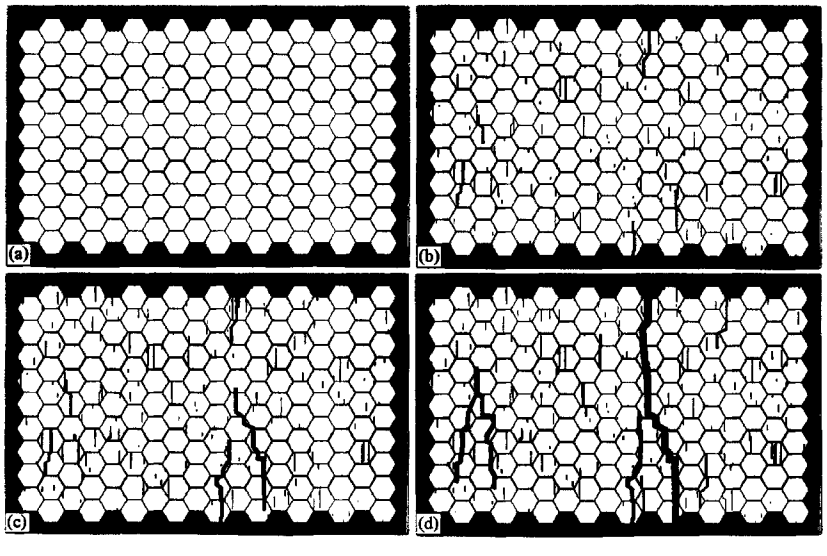

Simulation displays of the short-crack evolution process (vertical crack orientation): (*a*) initial stage of grain background, time step 0; (*b*) a few cracks across grain boundaries by coalescence, time step 9; (*c*) crack growth together with formation of main cracks, time step 10; (*d*) failure by growth and linkage of main cracks, time step 12.

Fig. 10

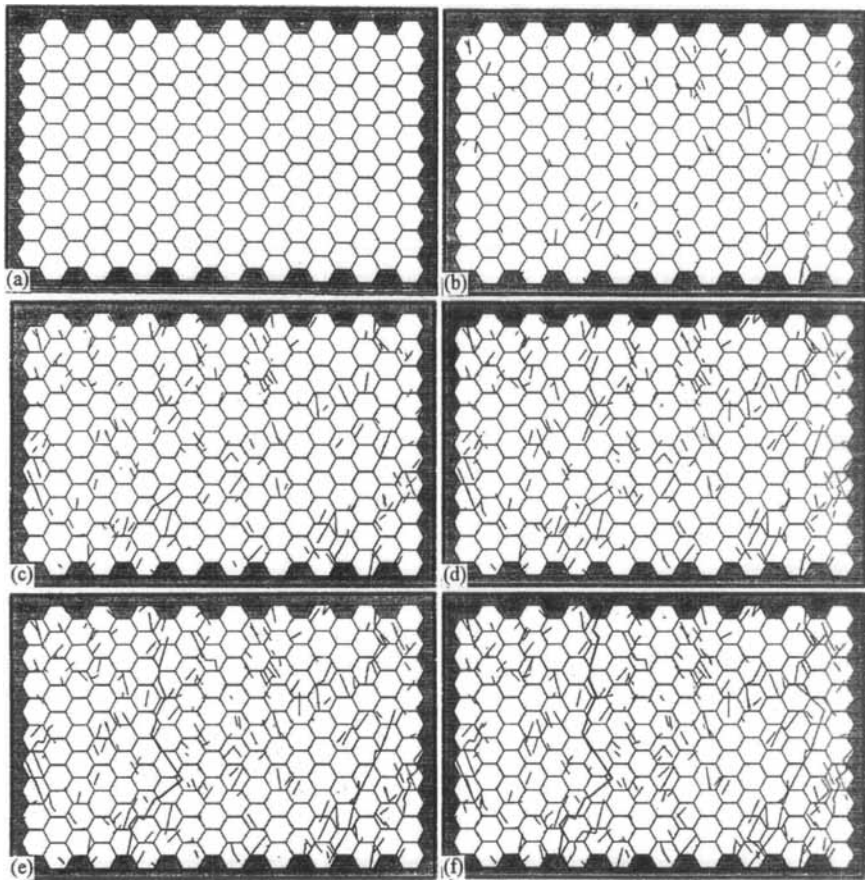

Simulation displays of short-crack evolution process (dispersed crack orientation): (*a*) initial stage of grain background, time step 0; (*b*) randomly produced cracks in grain domains, time step 3; (*c*) a few cracks across grain boundaries by coalescence, time step 9; (*d*) formation of several main cracks together with the multiplication of short cracks, time step 10; (*e*) growth and linkage of main cracks, time step 11; (*f*) a main crack running through the whole section, time step 12.

$$\log L = \log L_0 - (D_F - 1) \log \eta, \tag{9}$$

where L is the measured length of crack, η the measuring unit, and L_0 a constant. If $\log L$ and $\log \eta$ are linearly related, then the fractal dimension of concerned crack path can be obtained from the slope of the linear relation.

The second parameter is P_c, the critical value of percolation at failure. This is defined as the ratio of the number A_c of the pixels occupied by cracks to the A_t of total pixels:

$$P_c = \frac{A_c}{A_t}. \tag{10}$$

For the final stage of each simulation, that is a main crack runs through the whole section such as fig. 9(*d*) and fig. 10(*f*), the values of P_c and D_F can be calculated. After 700 simulations with type II crack orientation, we obtained 700 datum sets of P_c and D_F. Figure 11 shows the result of D_F distribution, indicating that the value of D_F is relatively stable with a sharp peak at $D_F = 1{\cdot}033$ and most datum points within the range between 1·03 and 1·05. The average value of D_F is 1·041 which is close to our previous experimental measurements (Hong *et al.* 1991). The fractal characteristics reflect the extent of crack deflection, which is attributed to the obstacle effect of grain boundary on crack growth. The histogram of P_c shown in fig. 12 shows another aspect of the distribution. Evidently, the value of P_c occurs in a wide range between 1·5% and 4·0%, with an outline shape of normal distribution. The average value of P_c is 2·65% and the peak value of N_i/N_t is only 5%. This indicates that the failure induced by short-crack evolution is a process with strong sensitivity to damage site arrangement. In other words, for a certain situation of damage site arrangement of short cracks, only a small amount of total damage is required to cause final failure. However, at the other extreme of damage site arrangement for short cracks, a large amount of total damage that is 2·6 times the amount in the former situation is needed for the failure. Therefore it is of great interest that the development of short cracks is closely related to the pattern of damage site distribution, which is regarded as an important feature of the collective evolution of short cracks.

In the present case of low-carbon steel, the percentage of pearlite is 16%, which is relatively small compared with that of medium-carbon structural steels. Experimental observations of the weld low-carbon steel indicated that, although

Fig. 11

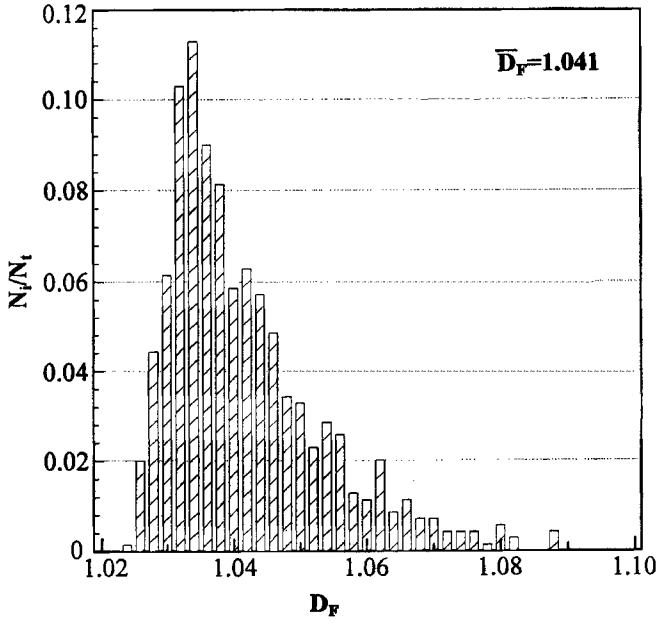

Relationship between fractal dimension D_F and N_i/N_t : N_i, number of events $(D_F)_i$; N_t, total number of events (700).

Fig. 12

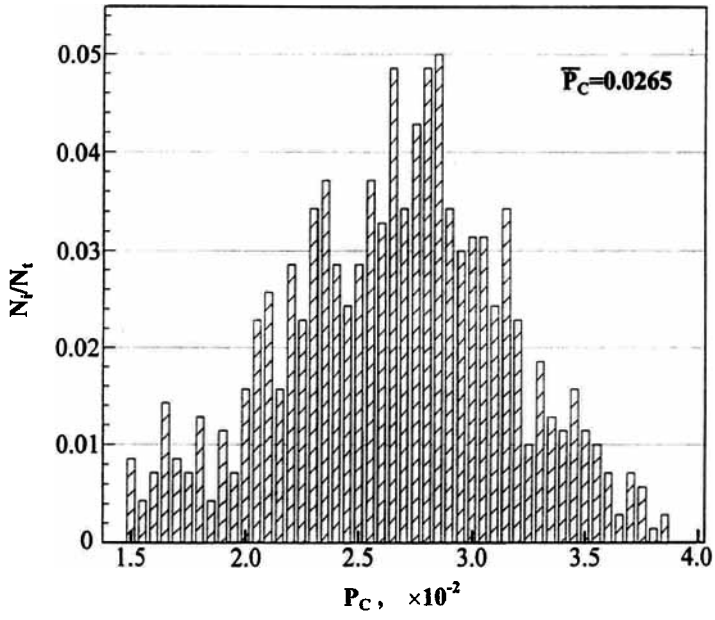

Relationship between critical value of percolation P_c and Ni/N_t : N_i, number of events at $(P_c)_i$; N_t, total number of events (700).

the ferrite–pearlite interface may also act as obstacles against crack propagation, the ferrite grain boundaries are the dominant barriers to short-crack growth. In a separate study of medium-carbon alloy steels, the effect of the ferrite–pearlite interface on short-crack behaviour will be further evaluated.

§ 5. Conclusions

The following conclusions are drawn from the present investigation of short-fatigue-crack behaviour in a weld low-carbon steel.

(1) The progression of short-fatigue-crack damage is a collective evolution process which is typified by the gradual increase in crack number per unit area with increasing number of fatigue cycles. The final failure is caused by the damage localization with the development of main cracks.
(2) Randomly dispersed short cracks possess an orientation preference, which is associated with the orientation factor of the related slip system.
(3) The computer simulation conducted in this investigation takes into account both the obstacle effect of grain boundaries and the crack orientation preference observed in the experiments. The resultant displays imitate the appearance of the collective evolution process of short cracks.
(4) The results of 700 simulations show that the value of fractal dimensions for cross-section cracks is relatively stable and that the critical value of percolation at failure covers a wide datum band, suggesting that the collective evolution of short cracks possesses a strong sensitivity to different damage site patterns.

ACKNOWLEDGEMENTS

This paper was supported by the National Natural Science Foundation of China, the National Outstanding Youth Scientific Award of China, and the Chinese Academy of Sciences.

REFERENCES

FATHULLA, A., WEISS, B., and STICKLER, R., 1986, *The Behaviour of Short Fatigue Cracks*, edited by K. J. Miller and E. R. de los Rios (London: Mechanical Engineering Publisher), p. 115.

HONG, Y.-S., LU, Y.-H., and ZHENG, Z.-M., 1989, *Fatigue Fract. Engng Mater. Struct.*, **12**, 323; 1990, *Acta metall. Sinica (Eng. Edn)* A, **3**, 276; 1991, *J. Mater. Sci.*, **26**, 1821.

LANKFORD, J., 1982, *Fatigue Engng Mater. Struct.*, **5**, 233.

LANKFORD, J., DAVIDSON, D. L., and CHAN, K. S., 1984, *Metall. Trans.* A, **15**, 1579.

NAVARRO, A., and DE LOS RIOS, E. R., 1988a, *Phil. Mag.* A, **57**, 15; 1988b, *Ibid.*, **57**, 37; 1988c, *Ibid.*, **57**, 43.

PANDE, C. S., RICHARDS, L. E., LOUAT, N., DEMPSEY, B. D., and SCHWOEBLE, A. J., 1987, *Acta metall.*, **35**, 1633.

PRICE, C. E., 1988, *Fatigue Fract. Engng. Mater. Struct.*, **11**, 483.

PRICE, C. E., and HENDERSON, G. W., 1988, *Fatigue Fract. Engng Mater. Struct.*, **11**, 493.

PRICE, C. E., and HOUGHTON, N. R., 1988, *Fatigue Fract. Engng. Mater. Struct.*, **11**, 501.

ROMANIV, O, N., SIMINKOVICH, V. N., and TKACH, A. N., 1982, *Fatigue Thresholds*, Vol. 2, edited by J. Backlund, A. F. Blom and C. J. Beevers (Warley, West Midlands: Engineering Materials Advisory Service), p. 799.

SUH, C. M., LEE, J. J., KANG, Y. G., AHN, H. J., and WOO, B. C., 1992, *Fatigue Fract. Engng Mater. Struct.*, **15**, 671.

TANAKA, K., HOJO, M., and NAKAI, Y., 1983, *Fatigue Mechanisms: Advances In Quantitative Measurement of Physical Damage*, ASTM Special Technical Publication No. 811 edited by J. Lankford, D. L. Davidson, W. L. Morris and R. P. Wei (Philadelphia, Pennsylvania: American Society for Testing and Materials), p. 207.

ZUREK, A. K., JAMES, M. R., and MORRIS, W. L., 1983, *Metall. Trans.* A, **14**, 1697.